AIAA JOURNAL
Vol. 41, No. 1, January 2003

High-Order Analysis of Unidirectional Sandwich Panels with Piezolaminated Face Sheets and Soft Core

Oded Rabinovitch* and Jack R. Vinson†
University of Delaware, Newark, Delaware 19716
and
Yeoshua Frostig‡
Technion—Israel Institute of Technology, 32000 Haifa, Israel

The bending behavior of unidirectional sandwich panels ("wide" or "narrow" beams) with a compressible "soft" core and piezoelectric active face sheets is investigated. The panels studied consist of composite face sheets with embedded active piezoelectric layers and a compressible core. The mathematical formulation adopts the principles of the high-order sandwich panel theory. The field equations and the boundary and continuity conditions are derived through the variational principle of virtual work, and the electromechanical effect is introduced using the linear piezoelectric constitutive equations. Higher-order effects due to flexibility of the core are incorporated in the analysis as a result of the solution of the field equations and are not presumed a priori. Numerical results are presented for typical cases of active sandwich panels and the effectiveness of various electrical actuation schemes is investigated. The effects associated with using piecewise continuous active layers are also investigated and discussed. The results reveal the capabilities of the proposed model and highlight some of the problems involved with the analysis and design of active sandwich panels.

Introduction

PIEZOELECTRIC actuation has become an accepted approach for shape control of many types of structural members. The implementation of such piezoelectric actuators in modern sandwich structures, which consist of composite laminated face sheets and a compressible "soft" core, combines the advantages of the lightweight structure and the embedded actuator. This configuration has additional advantages due to the protection that the soft core provides to the brittle piezoelectric materials and especially to piezoceramic materials such as lead–zirconia–titanate (PZT).

The static and dynamic behavior of active sandwich panels has been widely investigated in recent years. Wang and Quek[1] studied the flexural vibrations of sandwich beams with piezoelectric actuators, assuming an Euler-type model. Such assumption was also adopted by Abramovich and Pletner[2] for modeling the dynamic shape control of aluminum-PZT-foam sandwich beams. Trindade et al.[3] and Benjeddou et al.[4,5] assumed a piecewise linear deformation pattern through the depth of each layer of the sandwich structure, thus allowing shear deformation and shear actuation of the core. Bisegna and Caruso[6] adopted the Mindlin plate theory for the derivation of a finite element model for the active sandwich plate. A similar model for the piezoelectric shear actuation of sandwich panels and plates has been presented by Zhang and Sun.[7,8] This model uses the classical plate theory for the representation of the face sheets, whereas the core is assumed to be a first-order shear deformable plate. Although the approach used in Refs. 3–8 is suitable for the analysis of sandwich panels with incompressible core materials, it can not describe the localized effects that characterize sandwich panels with soft cores.

A different category of active sandwich panels has been investigated by Wang et al.,[9] Birman,[10] and Birman and Simonyan.[11] This type of application focus on piezoelectric actuation of the face sheets using surface-mounted or embedded active layers. The models derived in Refs. 10 and 11 neglect the longitudinal stresses in the core; thus, they imply the use of soft core materials. However, the vertical normal stresses in the core and its compressibility in the vertical direction are also neglected. These models also focus on midplane symmetric panels with symmetric distribution of the active layers and do not account for more general configurations.

In this paper, the bending behavior of a unidirectional sandwich panel ("wide" or "narrow" beam) with piezoelectrically active face sheets and a flexible core is investigated. The mathematical model presented follows the concepts of the high-order sandwich panel theory (HOSPT),[12–16] which is extended here to include the effect of the active piezocomposite layers. The accuracy of the theory and its ability to describe the stress concentration associated with the behavior of such a panel quantitatively have been demonstrated through comparison with photoelastic experimental results by Thomsen and Frostig.[17] The sandwich panels studied here consist of composite laminated face sheets with embedded or surface-mounted piezoceramic (PZT) layers and a soft core. The core is considered as a two-dimensional linear elastic medium that has shear and vertical normal resistance, whereas its longitudinal stresses are neglected. The face sheets are considered as membrane and bending members made of composite laminated materials and follow the Bernoulli–Euler assumption. The behavior of the active layers is governed by the linear piezoelectric constitutive equations, and they are activated with a prescribed electric field that is assumed uniform through their thickness and that coincides with the electrical poling direction. It is also assumed that the displacements are uniform through the width of the panel and that perfect bonding exists between the layers; thus, the interfaces maintain compatibility of deformations and resist vertical normal and shear stresses.

The mathematical formulation uses the principle of virtual work for the derivation of the field equations, along with the boundary and continuity conditions. It also included the generalized piezoelectric constitutive relations, the closed-form stress and deformation fields of the core, the governing equations, and their analytical solution. Numerical results in terms of deformations, stresses, and stress resultants are presented for some typical cases of active sandwich panels. The effectiveness of various actuation schemes and the effects associated with using piecewise piezoelectric actuators

Received 15 February 2002; revision received 15 July 2002; accepted for publication 29 July 2002.

*Postdoctoral Fellow, Center for Composite Materials; currently Senior Lecturer, Faculty of Civil and Environmental Engineering, Technion—Israel Institute of Technology, Technion City, 32000 Haifa, Israel; cvoded@techunix.technion.ac.il.

†H. Fletcher Brown Professor of Mechanical and Aerospace Engineering and the Center for Composite Materials. Fellow AIAA.

‡Professor, Faculty of Civil and Environmental Engineering.

are also investigated. The paper closes with a summary and some recommendations for the analysis and design of such active sandwich structures.

Mathematical Formulation

The mathematical formulation includes the derivation of the field equations and the boundary and continuity conditions, the constitutive relations, the stress and deformations fields of the core, the governing equations, and their analytical solution. The geometry, notation, and sign conventions appear in Fig. 1. The field equations and the boundary and continuity conditions are derived using the principle of virtual work that requires

$$\delta[H(\varepsilon, \bar{E}) + W] = 0 \tag{1}$$

where W is the potential of the external loads, H is the electrical enthalpy,[18] and δ is the variational operator. The first variation of the electrical enthalpy, stated in terms of the electric field, electric displacements, stresses, and strains is

$$\delta H(\varepsilon, \bar{E}) = \int_{v_t} \sigma^t_{xx}\delta\varepsilon^t_{xx}\,\mathrm{d}v_t + \int_{v_b} \sigma^b_{xx}\delta\varepsilon^b_{xx}\,\mathrm{d}v_b + \int_{v_c} (\tau_{xz}\delta\gamma_{zx} + \sigma_{zz}\delta\varepsilon_{zz})\,\mathrm{d}v_c - \int_{v_t} D^t\delta\bar{E}^t\,\mathrm{d}v_t - \int_{v_b} D^b\delta\bar{E}^b\,\mathrm{d}v_b \tag{2}$$

where σ^i_{xx} and ε^i_{xx} are the longitudinal stresses and strains in the upper, $i = t$, and lower, $i = b$, face sheets, respectively; τ_{xz} and γ_{zx} are the shear stress and shear angles in the core; σ_{zz} and ε_{zz} are the normal stresses and strains in the vertical direction of the core; D^i and $\bar{E}^i$ are the electrical displacements and the electrical fields of the upper, $i = t$, and lower, $i = b$, face sheets, respectively; v_i, $i = t, b, c$, are the volume of the upper and lower face sheets and the core, respectively; and $\mathrm{d}v_i$ is the infinitesimal volume element. Note that in the case of piezoelectric actuation, the electric field $\bar{E}$ is prescribed and the term $\delta\bar{E}$ vanishes.

The first variation of the potential energy of the surface loads and charges is

$$\delta W = -\int_{x=0}^{x=L} (n_t\delta u_{0t} + q_t\delta w_t + m_t\delta\beta_t)\,\mathrm{d}x - \int_{x=0}^{x=L} (n_b\delta u_{0b} + q_b\delta w_b + m_b\delta\beta_b)\,\mathrm{d}x + \int_{x=0}^{x=L} (\bar{\sigma}_t\delta\bar{\varphi}_t)\,\mathrm{d}x + \int_{x=0}^{x=L} (\bar{\sigma}_b\delta\bar{\varphi}_b)\,\mathrm{d}x - \sum_{j=1}^{NC_t}\int_{x=0}^{x=L} (\bar{N}_{tj}\delta u_{0t} + \bar{P}_{tj}\delta w_t + \bar{M}_{tj}\delta\beta_t)\delta_D(x - x_j)\,\mathrm{d}x - \sum_{j=1}^{NC_b}\int_{x=0}^{x=L} (\bar{N}_{bj}\delta u_{0b} + \bar{P}_{bj}\delta w_t + \bar{M}_{bj}\delta\beta_b)\delta_D(x - x_j)\,\mathrm{d}x \tag{3}$$

where u_{0i}, w_i, and β_i are the longitudinal and vertical displacements and the rotations of the reference level of the face sheets, respectively; n_i, q_i, and m_i are the distributed axial and transverse external loads and the distributed bending moments; $\bar{\sigma}_i$ are the surface charges multiplied by the width of the panel; $\bar{\varphi}_i$ are the electric potentials; $\bar{N}_{ij}$, $\bar{P}_{ij}$, and $\bar{M}_{ij}$, $i = t, b$, are the concentrated axial and transverse external loads and the concentrated bending moments exerted at $x = x_j$, respectively; δ_D is the Dirac function; and NC_i is the number of concentrated loads. Here again, the piezoelectric actuation is associated with prescribed electric field and potential; hence, the terms $\delta\bar{\varphi}_i$ also vanish.

Adopting the Bernoulli–Euler assumption along with the assumptions of negligible shear deformations and uniform deflections through the width of the panel, the displacement fields of the upper and lower face sheets take the following forms:

$$w_i(x, y, z) = w_i(x) \tag{4a}$$

$$u_i(x, y, z) = u_{0i}(x) + z_i\beta_i(x) \tag{4b}$$

$$\beta_i(x) = -w_{i,x}(x) \qquad (i = t, b) \tag{4c}$$

where z_i, $i = t, b$, is measured from the midplane of each face sheet downward, independently, and $(\,)_{,j}$ denotes the derivative with respect to the coordinate j. Equations (4a–4c), along with the assumption of small deformation, yield the following kinematic relations for the face sheets:

$$\varepsilon^i_{xx} = u_{0i,x} - z_i \cdot w_{i,xx} \tag{5a}$$

$$\varepsilon^i_{xx0} = u_{0i,x} \tag{5b}$$

$$\chi^i_{xx} = \beta_{i,x} = -w_{i,xx} \qquad (i = t, b) \tag{5c}$$

where ε^i_{xx0} and χ^i_{xx} are the midplane strains and curvatures of the face sheets, respectively.

The kinematic relations of the core are based on linear two-dimensional elasticity and read

$$\gamma_{xz} = u_{c,z}(x, z_c) + w_{c,x}(x, z_c) \tag{6a}$$

$$\varepsilon_{zz} = w_{c,z}(x, z_c) \tag{6b}$$

where u_c and w_c are the longitudinal and vertical displacements of the core, respectively, and z_c is the vertical coordinate of the core, measured from the upper core–face-sheet interface downward. Note that, as opposed to the displacements fields of the face sheets, which

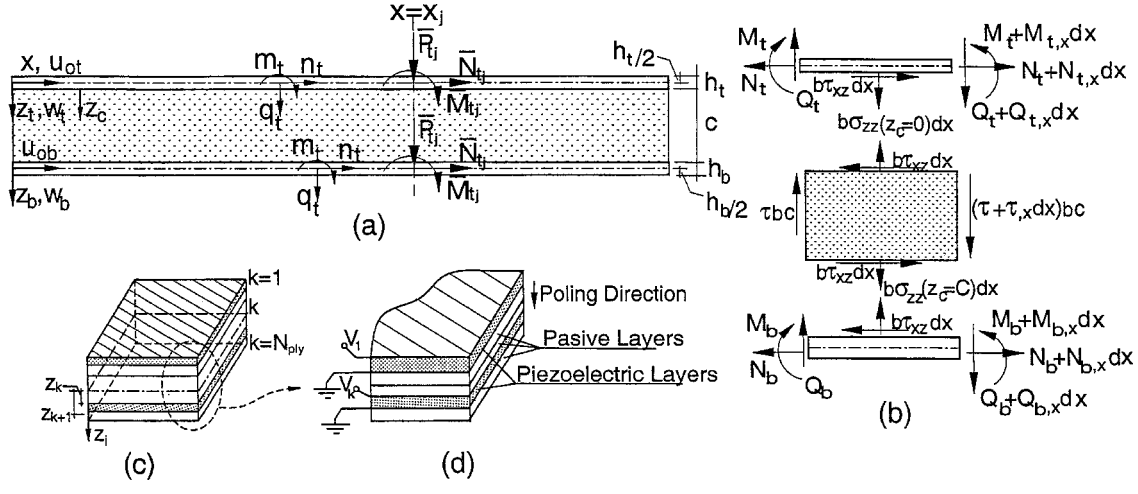

Fig. 1 Notations and sign conventions: a) geometry, coordinate systems, deflections and external loads; b) stresses and stress resultants; c) layup of piezocomposite upper and lower face sheets; and d) applied voltage and electric poling field for piezocomposite face sheets.

adopt the Bernoulli–Euler assumption [Eqs. (4)], no assumptions are made with regard to the displacement fields of the core.

The requirement for perfect bonding of the core to the face sheets yields the following compatibility conditions at the upper and lower core–face-sheet interfaces:

$$w_c(x, 0) = w_t(x) \tag{7a}$$

$$w_c(x, c) = w_b(x) \tag{7b}$$

$$u_c(x, 0) = u_t(x, h_t/2) = u_{0t}(x) - (h_t/2)w_{t,x}(x) \tag{8a}$$

$$u_c(x, c) = u_b(x, -h_b/2) = u_{0b}(x) + (h_b/2)w_{b,x}(x) \tag{8b}$$

Note that $z_c = 0$ and $z_c = c$ denote the upper and lower face-sheet–core interfaces, respectively, and h_i, $i = t, b$, are the thicknesses of the top and bottom face sheets, respectively.

The internal stress resultants are defined by integration of stresses through the thickness of each face sheet and read

$$N^i_{xx} = \int_{-h_i/2}^{h_i/2} \sigma^i_{xx}\, \mathrm{d}z_i \tag{9a}$$

$$M^i_{xx} = \int_{-h_i/2}^{h_i/2} \sigma^i_{xx} z_i\, \mathrm{d}z_i \tag{9b}$$

When the definitions of the internal stress resultants, along with the kinematic relations and the compatibility conditions, are introduced into the variational principle, and by the use of the fundamental lemma of the calculus of variations,[19] the following field equations for the face sheets and the core are obtained:

$$N^t_{xx,x} + b\tau_{xz}(x, 0) + n_t = 0 \tag{10}$$

$$N^b_{xx,x} - b\tau_{xz}(x, c) + n_b = 0 \tag{11}$$

$$M^t_{xx,xx} + (bh_t/2)\tau_{xz,x}(x, 0) + b\sigma_{zz}(x, 0) + q_t - m_{t,x} = 0 \tag{12}$$

$$M^b_{xx,xx} + (bh_b/2)\tau_{xz,x}(x, c) - b\sigma_{zz}(x, c) + q_b - m_{b,x} = 0 \tag{13}$$

$$\sigma_{zz,z} + \tau_{xz,x} = 0 \tag{14}$$

$$\tau_{xz,z} = 0 \tag{15}$$

The boundary conditions at $x = 0$ or L, which are also derived by the use of the variational principle, take the following form for the various face sheets, $i = t, b$:

$$\lambda N^i_{xx} - \bar{N}_i = 0 \qquad \text{or} \qquad u_{0i} = \bar{u}_{0i} \tag{16}$$

$$\lambda\left[M^i_{xx,x} + (bh/2)\tau_{xz} - m_i\right] - \bar{P}_i = 0 \qquad \text{or} \qquad w_i = \bar{w}_i \tag{17}$$

$$-\lambda M^i_{xx} + \bar{M}_i = 0 \qquad \text{or} \qquad w_{i,x} = \bar{w}_{i,x} \tag{18}$$

$$\tau_{xz}(x, z_c) = 0 \qquad \text{or} \qquad w_c(x, z_c) = \bar{w}_c(z_c) \tag{19}$$

where $\lambda = 1$ at $x = L$ and $\lambda = -1$ at $x = 0$; $\bar{N}_i$, $\bar{P}_i$, and $\bar{M}_i$ are external concentrated loads and bending moments exerted at the ends of the face sheets; and $\bar{u}_{0i}$, $\bar{w}_i$, and $\bar{w}_{i,j}$ are prescribed deformations and rotations at the ends of the upper, $i = t$, and the lower, $i = b$, faces, respectively.

The continuity conditions for the various face sheets, $i = t, b$, at any point $x = x_j$ within the panel requires continuity of the displacements and slopes, as well as equilibrium of the internal stress resultants and the imposed concentrated loads, as follows:

$$u^{(-)}_{0i} = u^{(+)}_{0i} \tag{20}$$

$$w^{(-)}_i = w^{(+)}_i \tag{21}$$

$$w^{(-)}_{i,x} = w^{(+)}_{i,x} \tag{22}$$

$$N^{i(-)}_{xx} - N^{i(+)}_{xx} = \bar{N}_{ij} \tag{23}$$

$$-M^{i(-)}_{xx} + M^{i(+)}_{xx} = \bar{M}_{ij} \tag{24}$$

$$M^{i(-)}_{xx,x} + \left(bh^{(-)}_i/2\right)\tau^{(-)}_{xz} - m^{(-)}_i - M^{i(+)}_{xx,x} - \left(bh^{(+)}_i/2\right)\tau^{(+)}_{xz} + m^{(+)}_i = \bar{P}_{ij} \tag{25}$$

The continuity conditions of the core are

$$\tau^{(-)}_{xz}(x, z_c) = \tau^{(+)}_c(x, z_c) \tag{26}$$

$$w^{(-)}_c(x, z_c) = w^{(+)}_c(x, z_c) \tag{27}$$

where the superscripts $(-)$ and $(+)$ denote quantities left and right to the point $x = x_j$, respectively.

The constitutive relations for the face sheets use the classical lamination theory and the linear piezoelectric constitutive equations (the converse piezoelectric effect). In the case of wide beam conditions, $\varepsilon^k_{yy} = \gamma^k_{yz} = \gamma^k_{xy} = 0$, the constitutive relations are

$$\sigma^k_{xx} = c^k_{11}\varepsilon^k_{xx} - e^k_{31}\bar{E}^k_3 \tag{28a}$$

$$D^k_3 = e^k_{31}\varepsilon^k_{xx} + \kappa^k_{33}\bar{E}^k_3 \tag{28b}$$

where e^k_{31} is the transformed piezoelectric stress coefficient of the kth layer within the upper or lower face sheet; κ_{33} is the electrical permittivity of that lamina; c^k_{11} is its stiffness; $\bar{E}^k_3$ is the electric field; and the 1 and 3 directions coincide with the face sheet's coordinates x, and z_i, $i = t, b$, respectively. For the passive layers within the laminated face sheets, all of the piezoelectric constants vanish, and Eq. (28a) yields to the classical Hooke's law.

From the definition of the electric field being the negative gradient of the potential, and by the use of the assumption of uniform field through the thickness of the active layer and the sign conventions of Fig. 1, the expression for he electric field as the kth layer is

$$\bar{E}^k_3 = -[V_k/(z_k - z_{k-1})] \tag{29}$$

where V_k is the voltage applied through the thickness of the kth layer.

Integration of the constitutive equations through the thickness of each face sheet yields the constitutive relations for the upper and lower active face sheets, as follows:

$$\begin{bmatrix} N^i_{xx} \\ M^i_{xx} \end{bmatrix} = \begin{bmatrix} A^i_{11} & B^i_{11} \\ B^i_{11} & D^i_{11} \end{bmatrix} \begin{bmatrix} \varepsilon^i_{xx0} \\ \chi^i_{xx} \end{bmatrix} - \begin{bmatrix} N^i_{\mathrm{PZ}} \\ M^i_{\mathrm{PZ}} \end{bmatrix} \qquad (i = t, b) \tag{30}$$

where A^i_{11}, B^i_{11}, and D^i_{11} are the rigidities of the upper $(i = t)$ and lower $(i = b)$ face sheets multiplied by the width of the panel b and N^i_{PZ} and M^i_{PZ} are the induced piezoelectric forces and couples defined by

$$\begin{bmatrix} N^i_{\mathrm{PZ}} \\ M^i_{\mathrm{PZ}} \end{bmatrix} = b\sum_{k=1}^{N_{\mathrm{ply}}} \int_{z_{k-1}}^{z_k} e^k_{31}\bar{E}_3 \begin{bmatrix} 1 \\ z_i \end{bmatrix} \mathrm{d}z_i \tag{31}$$

where N_{ply} is the number of layers within each face sheet.

The constitutive relations for the core follow Hooke's law and read

$$\tau_{xz} = G_c \cdot \gamma_{xz}, \qquad \sigma_{zz} = E_c \cdot \varepsilon_{zz} \tag{32}$$

where G_c is the shear modulus of the core and E_c is the elastic modulus of the core in the vertical direction.

The stress and displacement fields of the core are derived by solving the field equations, Eqs. (14) and (15); along with the kinematic and constitutive relations, Eqs. (6) and (31); and the compatibility conditions at the upper and the lower face core interfaces, Eqs. (7) and (8). This solution procedure yields the following closed-form expressions:

$$\tau_{xz}(x, z_c) = \tau_{xz}(x) = \tau \tag{33}$$

$$\sigma_{zz}(x, z_c) = -\tau_{,x}(2z_c - c)/2 + E_c(w_b - w_t)/c \tag{34}$$

$$w_c(x, z_c) = -\tau_{,x}(z_c - c)z_c/2E_c + (w_b - w_t)z_c/c + w_t \tag{35}$$

$$u_c(x, z_c) = \tau z_c/G_c - (\tau_{,xx}/2E_c)\left(z_c^2 c/2 - z_c^3/3\right) - w_{b,x} z_c^2/c - w_{t,x}\left(-z_c^2/2c + z_c + h_t/2\right) + u_{0t} \tag{36}$$

Equations (33–36) reveal the high-order stress and displacement fields of the core, which are a result of the solution of its field equations and are not presumed a priori.

Because of the limited size of available piezoceramic layers, piecewise piezoelectric actuators are used in many practical applications. In this case, the gap between every two adjacent active layers yields rapid changes in the thickness of the core. Thus, the integral term of the continuity conditions of the core at $x = x_j$ reads

$$\int_{z_c=0}^{z_c=c^{(-)}} \tau^{(-)} \cdot \delta w_c^{(-)}(x_j, z_c)\, \mathrm{d}z_c = \int_{z_c=0}^{z_c=c^{(+)}} \tau^{(+)} \cdot \delta w_c^{(+)}(x_j, z_c)\, \mathrm{d}z_c \tag{37}$$

By the use of the shear stress distribution of Eq. (33), the integral continuity condition becomes

$$c^{(-)}\tau(x_j)^{(-)} \cdot \frac{1}{c^{(-)}} \int_{z_c=0}^{z_c=c^{(-)}} \delta w_c^{(-)}(x_j, z_c)\, \mathrm{d}z_c = c^{(+)}\tau(x_j)^{(+)} \cdot \frac{1}{c^{(+)}} \int_{z_c=0}^{z_c=c^{(+)}} \delta w_c^{(+)}(x_j, z_c)\, \mathrm{d}z_c \tag{38}$$

This continuity condition can be described by

$$c^{(-)}\tau^{(-)}(x_j) \cdot \delta w_{c,\text{average}}^{(-)}(x_j) = c^{(+)}\tau^{(+)}(x_j) \cdot \delta w_{c,\text{average}}^{(+)}(x_j) \tag{39}$$

where $\delta w_{c,\text{average}}$ is the averaged through the thickness vertical displacement. Hence, in the case of discontinuous core thickness, the continuity conditions of the core, Eqs. (26) and (27), are replaced by

$$c^{(-)}\tau^{(-)}(x_j) = c^{(+)}\tau^{(+)}(x_j) \tag{40}$$

$$w_{c,\text{average}}^{(-)}(x_j) = w_{c,\text{average}}^{(+)}(x_j) \tag{41}$$

The governing equations are stated in terms of the unknown displacements of the upper and the lower face sheets and the unknown shear stress of the core. The equations are derived by introducing the generalized constitutive relations, Eq. (31), along with the closed-form solution of the stress and displacement fields, Eqs. (33–36), into the four field equations of the face sheets, Eqs. (10–13). The fifth governing equation is a result of the requirement of compatible longitudinal displacement fields at $z_c = c$ [see Eq. (8b)]. After some algebraic manipulations, the governing equations of the active panel read

$$A_{11}^t u_{0t,xx} - B_{11}^t w_{t,xxx} + b\tau = N_{\text{PZ},x}^t - n^t \tag{42}$$

$$A_{11}^b u_{0b,xx} - B_{11}^b w_{b,xxx} - b\tau = N_{\text{PZ},x}^b - n^b \tag{43}$$

$$D_{11}^t w_{t,xxxx} - B_{11}^t u_{0t,xxx} + (bE_c/c)(w_t - w_b) - b\tau_{,x}(c + h_t)/2 = q^t - m_{,x}^t - M_{\text{PZ},xx}^t \tag{44}$$

$$D_{11}^b w_{b,xxxx} - B_{11}^b u_{0b,xxx} - (bE_c/c)(w_t - w_b) - b\tau_{,x}(c + h_b)/2 = q^b - m_{,x}^b - M_{\text{PZ},xx}^b \tag{45}$$

$$u_{0t} - u_{0b} - (c + h_t)w_{t,x}/2 - (c + h_b)w_{b,x}/2 - \tau_{,xx}c^3/12E_c + \tau c/G_c = 0 \tag{46}$$

Equations (42–46) form a 14th-order system of coupled ordinary differential equations. The linearity of the equations and the constant coefficients allows the use of the classical procedure of solving differential equations.[20] By the use of this procedure, the closed-form solution of Eqs. (42–46) takes the following form:

$$w_t = \sum_{i=1}^{8} \alpha_{wt,i} C_i \exp(s_i x) + C_9 + C_{10}x + C_{11}x^2 + C_{12}x^3 + w_t^p \tag{47}$$

$$w_b = \sum_{i=1}^{8} \alpha_{wb,i} C_i \exp(s_i x) + C_9 + C_{10}x + C_{11}x^2 + C_{12}x^3 + w_b^p \tag{48}$$

$$u_{0t} = \sum_{i=1}^{8} \alpha_{u0t,i} C_i \exp(s_i x) + \left\{ \frac{6cA_{11}^t A_{11}^b}{bG_c\left(A_{11}^t + A_{11}^b\right)} \left[\left(c + \frac{h_t}{2} + \frac{h_b}{2} + \frac{B_{11}^b}{A_{11}^b} - \frac{B_{11}^t}{A_{11}^t} \right) \right] C_{12} + \left(c + \frac{h_t}{2} + \frac{h_b}{2} \right) C_{10} + C_{13} \right\} + \left\{ 2\left(c + \frac{h_t}{2} + \frac{h_b}{2} \right) C_{11} + C_{14} \right\} x + \left\{ \frac{3}{\left(A_{11}^t + A_{11}^b\right)} \times \left[\left(c + \frac{h_t}{2} + \frac{h_b}{2} \right) A_{11}^b - B_{11}^b - B_{11}^t \right] C_{12} \right\} x^2 + u_{0t}^P \tag{49}$$

$$u_{0b} = \sum_{i=1}^{8} \alpha_{u0b,i} C_i \exp(s_i x) + C_{13} + C_{14}x + 3\left\{ \left(c + \frac{h_t}{2} + \frac{h_b}{2} \right) A_{11}^b + B_{11}^b + B_{11}^t \right\} C_{12}x^2 + u_{0b}^P \tag{50}$$

$$\tau = \sum_{i=1}^{8} \alpha_{\tau,i} C_i \exp(s_i x) - \left\{ \frac{6}{b\left(A_{11}^t + A_{11}^b\right)} \left[A_{11}^t A_{11}^b \left(c + \frac{h_t}{2} + \frac{h_b}{2} \right) + B_{11}^b A_{11}^t - B_{11}^t A_{11}^b \right] \right\} C_{12} + \tau^P \tag{51}$$

where s_i are the roots of the characteristic polynomial, $[\alpha_{wt,i}, \alpha_{wb,i}, \alpha_{u0t,i}, \alpha_{u0b,i}, \alpha_{\tau,i}]^T$ is the normalized eigenvector for the s_i root, the superscript P denotes the particular solution, and $C_1, \ldots, C_{14}$ are constants determined using the boundary conditions. Note that Eqs. (47–51) provide a closed-form solution of the governing equations, hence, the analysis is accurate within the bounds of the assumptions made. The accuracy of the approach used here, and its ability to provide quantitative description of the stress distributions in panels subjected to mechanical loads, has been demonstrated experimentally by Thomsen and Frostig.[17] The deformations, stress resultants, and stresses induced due to the piezoelectric actuation are investigated next.

Numerical Study

The numerical study focuses on two practical cases of active sandwich panels. The first case investigates and compares various schemes for the electrical actuation of cantilevered sandwich panels of various geometrical layouts. The second numerical case examines the behavior of a sandwich panel actuated using piecewise piezoelectric layers and compares it with the response of a panel actuated with continuous layers. In both cases, results in terms of deflections, stress resultants, and stresses are presented and discussed.

Case 1: Bending Actuation of Cantilevered Panels

The bending behavior of two cantilevered sandwich panels that differ in their geometrical layouts is investigated. The geometry of the panels appears in Fig. 2 and the mechanical properties of the various materials appear in Tables 1 and 2. The first long panel is characterized by a relatively large length-to-face-sheet-thickness

Table 1 Mechanical properties of the face sheet passive substrate and piezoceramic (PZT) layers

Lamina	E_1, MPa	E_2, MPa	G_{12}, MPa	υ_{12}	d_{31}, mm/V	d_{32}, mm/V	t, mm
Glass/epoxy	47,600	13,300	4,750	0.30	——	——	0.12
PZT	63,000	63,000	24,800	0.28	-270×10^{-9}	-270×10^{-9}	0.16

ratio ($L/h_t = 100$), and the second short panel is characterized by a smaller length-to-face-sheet-thickness ratio ($L/h_t = 25$). In all cases, a uniform aspect ratio of $L/c = 5$ is adopted for the core; the length to width ratio is $L/b = 2$; the stacking sequences for the passive glass/epoxy upper and lower face sheets are $[0, 90]_S$ and $[0_2, 90]_S$, respectively; and a dc voltage $V = 500$ V is used. The three investigated actuation schemes are described next.

Global Bending

The piezoceramic (PZT) layers that are located at the upper and lower faces of the upper face sheet are subjected to positive voltage, whereas the layers that are located at the upper and lower faces of the lower face sheet are subjected to negative voltage (see Fig. 2b). This scheme mainly induces global bending of the panel in the form of tensile/compressive forces at the face sheets.

Local Bending

In this case, the piezoceramic layers located at the upper faces of both face sheets are actuated with positive voltage, whereas the piezoceramic layers located at the lower faces of both face sheets are actuated with negative voltage (Fig. 2c). This scheme yields localized bending in the upper and the lower face sheets.

Table 2 Elastic moduli of the foam core material

Elastic modulus	Value
E_c, MPa	50
G_c, MPa	20

Nonsymmetric Actuation

In this scheme, the piezoelectric layers are located at the lower face of the upper face sheet and at the upper face of the lower face sheet (see Fig. 2d). The layer at the upper interface is actuated with negative voltage, whereas the piezoelectric layer at the lower interface is actuated with positive voltage. This configuration yields coupled in-plane and bending actuation, as well as stretching/bending rigidities in the face sheets. Note that the thickness of the piezoelectric layers and the applied voltage used in this scheme are twice the quantities used in the global and local bending schemes; hence, the total amount of the piezoelectric material and the electric field are kept uniform in all cases. Also note that, in this layout, the active layers are located at the inner faces of the face sheets; thus, the brittle piezoceramic layers are protected by the core, and a smaller number of surface electrodes are required.

The results for the various actuation schemes for the long panel appear in Figs. 3–5. The longitudinal and transverse displacements of the face sheets appear in Figs. 3a and 3b, respectively, and reveal that the global bending actuation (marked with superscript A) yields significantly larger deflections than the local bending scheme (marked with B) does. The curves also reveal that the nonsymmetric actuation (marked with C) yields deflections that are in the same order of magnitude as those induced in the global bending scheme. In addition, both the local bending and the nonsymmetric schemes are involved with localized deflections of the face sheets near the free edge. This effect is attributed to the localized bending effects at the edge of the panel and to the flexibility of the core. The longitudinal displacements at the free edge of the panel are plotted through the thickness of the entire cross section of the panel in Fig. 3c. The curves reveal the high-order effects that take the form of nonlinear displacement patterns through the depth of the core.

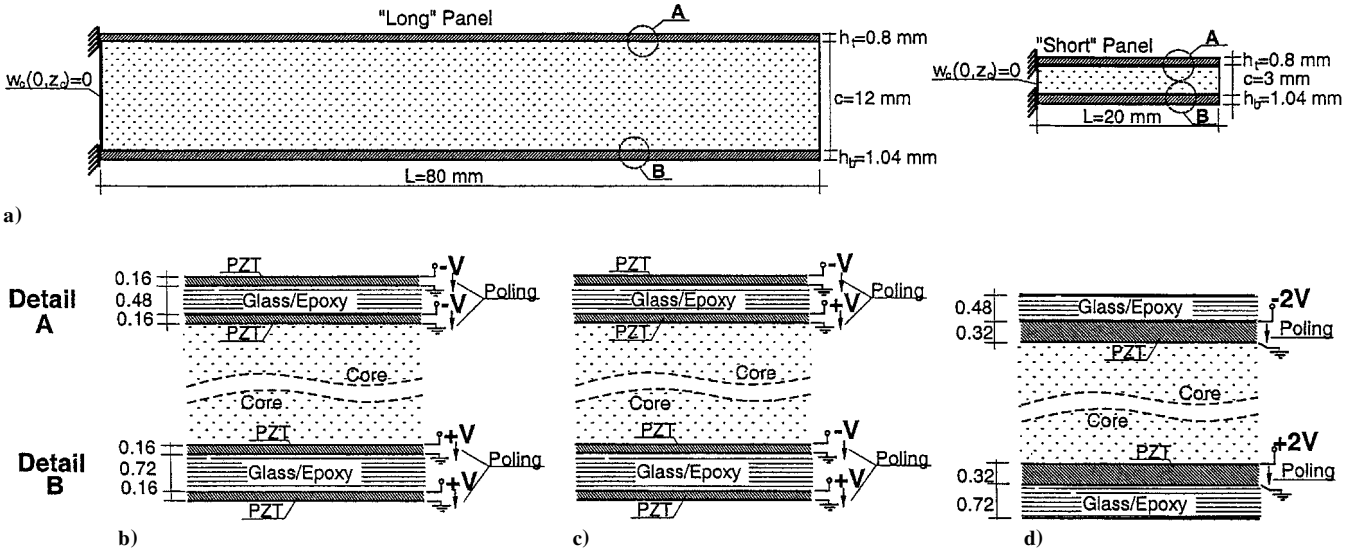

Fig. 2 Case 1, piezoelectric actuation of cantilevered sandwich panels: a) dimensions and geometry, b) global bending scheme, c) local bending scheme, and d) nonsymmetric scheme.

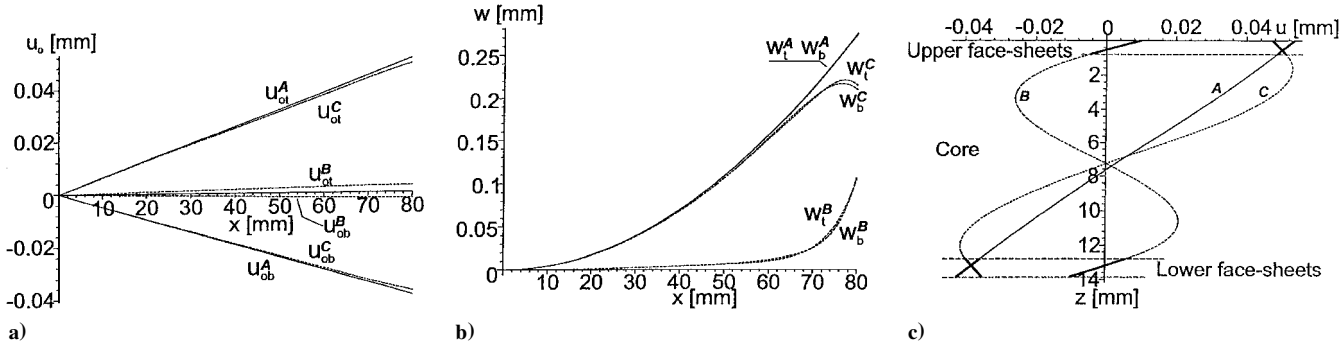

Fig. 3 Displacements in active long panel: a) longitudinal, b) vertical, and c) longitudinal displacement profiles at the free edge of the panel (A, global bending; B, local bending; and C, nonsymmetric actuation).

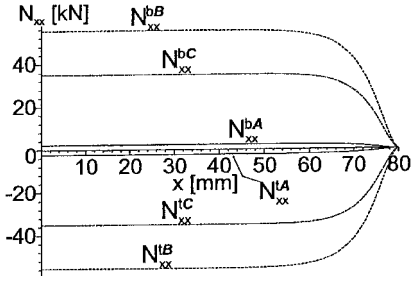
N_xx [kN]
N_xx^bB
N_xx^bC
N_xx^bA
N_xx^tA
N_xx^tC
N_xx^tB
40
20
0
-20
-40
10 20 30 40 50 60 70 80
x [mm]

a)

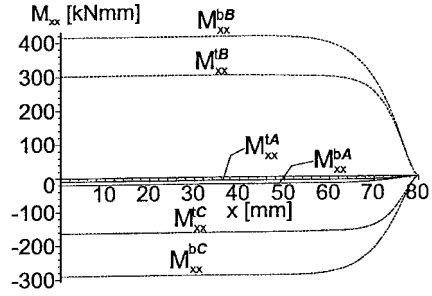
M_xx [kNmm]
M_xx^bB
M_xx^tB
M_xx^tA
M_xx^bA
M_xx^tC
M_xx^bC
400
300
200
100
0
-100
-200
-300
10 20 30 40 50 60 70 80
x [mm]

b)

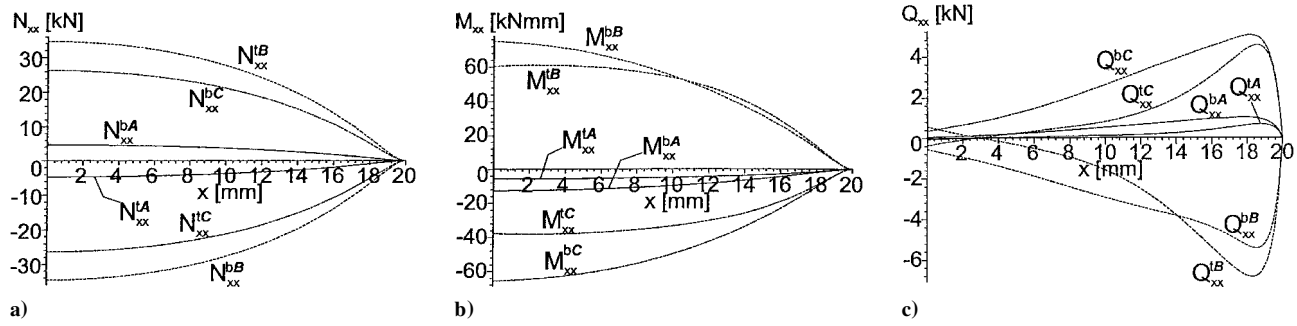

Fig. 7 Stress resultants in active short panel: a) axial forces, b) bending moments, and c) shear forces (*A*, global bending; *B*, local bending; and *C*, nonsymmetric actuation).

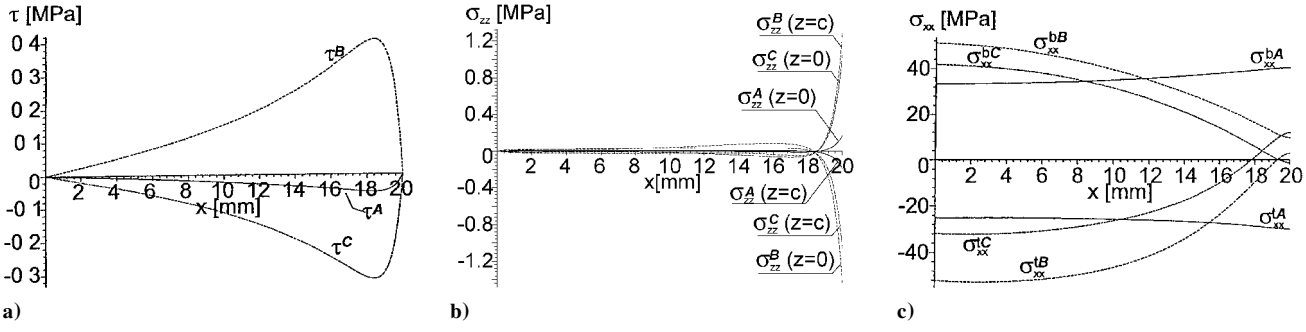

Fig. 8 Stresses in active short panel: a) shear stresses in the core, b) vertical normal stresses at the core–face-sheet interfaces, and c) longitudinal normal stresses at outer piezoelectric layers (*A*, global bending; *B*, local bending; and *C*, nonsymmetric actuation).

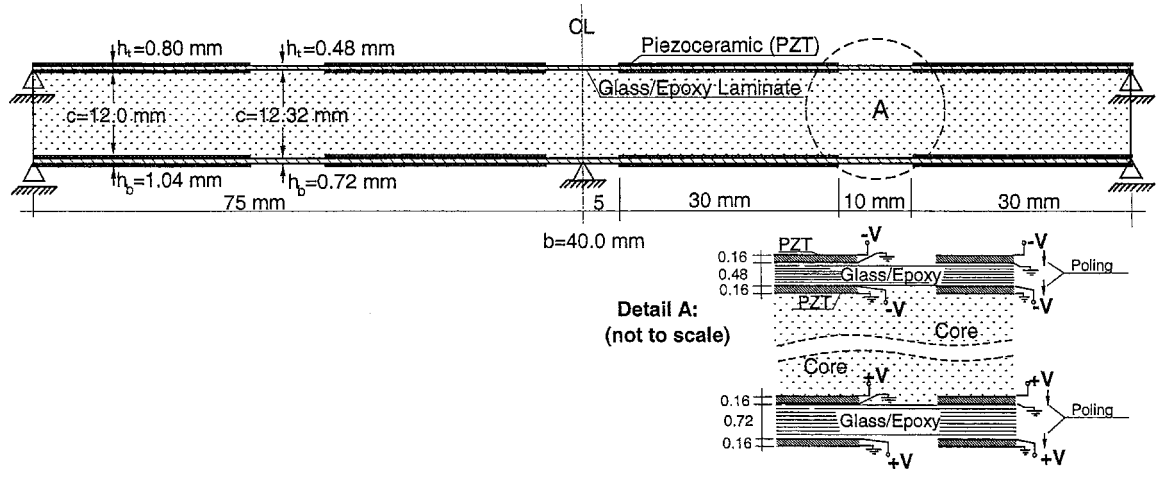

Fig. 9 Piezoelectric actuation with piecewise and continuous piezoceramic (PZT) layers.

sheets that occurs near the free edge of the panel. In the long panel, these phenomena decay within a distance of about one times the depth of the panel. Yet, in the short panel, they are more dominant and decay much slower.

The internal stress resultants in the short panel appear Figs. 7a–7c and reveal that the local bending actuation, which yields larger deflections and can, thus, be considered more effective, is also associated with increased internal stress resultants. The shear and vertical normal stresses in the core and the longitudinal stresses in the piezoelectric layers appear in Figs. 8a–8c, respectively, and indicate that the local bending scheme is associated with the highest stresses, whereas the global bending scheme is involved with the lowest ones. However, here again the longitudinal normal stresses are of the same order of magnitude for all cases. Hence, in the case of the short panel, the local bending scheme provides an adequate solution that combines the largest deflections with longitudinal normal stress that are not larger than those observed in the other configuration. Nevertheless, the design of such panels must account for the enhanced shear and vertical normal stresses associated with this scheme.

Case 2: Piezoelectric Actuation with Piecewise Active Layers

The second numerical case investigates the effect of using piecewise piezoelectric layers for the actuation of the sandwich panel. Such piecewise actuation is enforced in many practical cases due to the limited sizes and layouts of the piezoceramic active layers. The response of the panel actuated with the piecewise layers is investigated and compared with the behavior of a similar panel that is actuated with continuous layers. The mechanical properties, stacking sequences, and electrical actuation scheme of the panels are identical to those used in the global bending scheme (see Tables 1 and 2). The geometrical layout of the piecewise active panel appears in Fig. 9. The discontinuities in the piezoceramic layers, and the corresponding changes in the depth of the

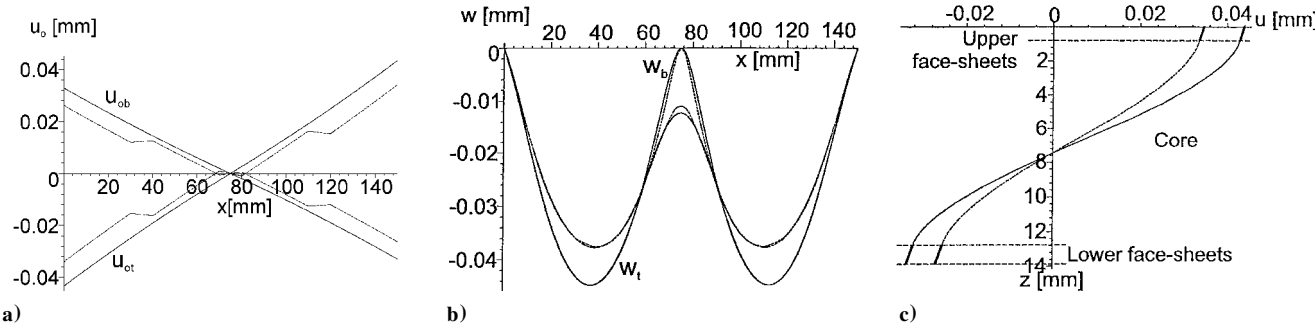

Fig. 10 Piezoelectric actuation with piecewise and continuous layers: a) longitudinal displacements, b) vertical deflections, and c) longitudinal displacement profiles at the free edge of the panel (——, continuous PZT and - - - -, piecewise PZT).

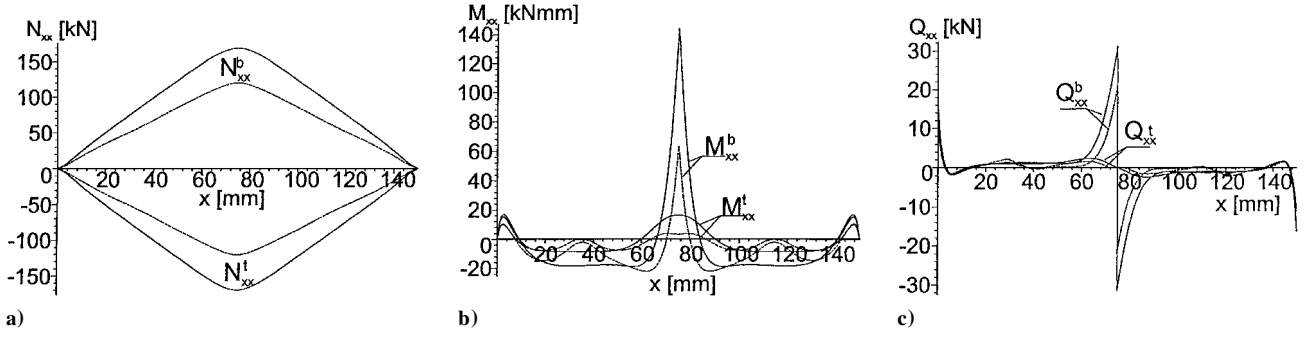

Fig. 11 Piezoelectric actuation with piecewise and continuous layers: a) axial forces, b) bending moments, and c) shear forces (——, continuous PZT and - - - -, piecewise PZT).

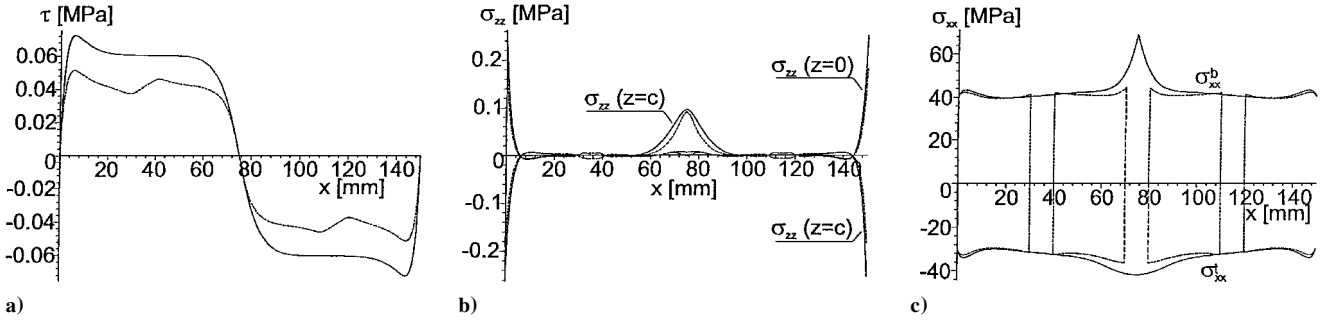

Fig. 12 Piezoelectric actuation with piecewise and continuous layers: a) shear stresses in the core, b) vertical normal stresses at the core–face-sheet interfaces, and c) longitudinal normal stresses at outer piezoelectric layers (——, continuous piezoelectric layers and - - - -, piecewise piezoelectric layers).

core, are modeled by the introduction of an additional passive region between every two active regions (see detail A in Fig. 9) and employment of the continuity conditions of Eqs. (20–25), (40), and (41).

The longitudinal and vertical displacement of the upper and lower face sheets and the longitudinal displacement profiles through the entire thickness of the panel at a section located at $x = 150$ mm appear in Figs. 10a–10c, respectively. The results indicate that the use of the piecewise piezoelectric layers reduces the achieved peak deflections by about 15–20% as compared to the continuous layers. Figure 10b also reveal the nonidentical deflections of the upper and the lower face sheets, especially near the inner support. These differences are attributed to the static indeterminacy of the panel, the reaction in the inner support, and the compressibility of the core.

Additional results in terms of the internal in-plane, bending, and shear stress resultants are presented in Figs. 11a–11c. These curves reveal that the magnitudes of the internal forces in the piecewise actuated panel are reduced by about 30–55% as compared to those for the continuous configuration. This effect is explained by the reduced overall stiffness of the panel due to the gaps between the piezoelectric layers. The shear stresses in the core, the vertical normal stresses in its interfaces, and the longitudinal stresses in the outer piezoceramic layers appear in Fig. 12. These results indicate that the piecewise actuation is associated with reduced shear stresses in the core; however, the peak vertical normal stresses are almost the same in both cases. The longitudinal normal stresses in the piezoceramic layers are also alike in both cases, excluding the close vicinity of the inner support, which is associated with higher stresses in the continuous configuration. Hence, locating the inner support within the gap between two adjacent active regions avoids exposing the piezoceramic layers to the stress concentration induced by the reaction.

Summary

A systematic high-order model for the local and overall analysis of sandwich panels with piezoelectric composite face sheets and a compressible core has been presented. The derived model follows the concept of the HOSPT and uses the piezoelectric generalized constitutive equations for the representation of the piezoelectric effects. The model accounts for arbitrary symmetric or nonsymmetric layup for the piezocomposite face sheets, as well as any combination of loads and boundary conditions. The core considered is compressible; thus, its height changes, and its plane of section does not remain in plane after deformations.

The field equations, as well as the corresponding boundary and continuity conditions, have been derived using the variational

principle of minimization of the electrical enthalpy and the potential of the surface tractions. The field equations, along with the constitutive relations, the closed-form stress and displacement fields of the core, and the compatibility requirements, yield a 14th-order system of ordinary differential equations that are solved analytically.

The capabilities of the proposed model have been demonstrated through a numerical study of two typical cases of active sandwich panels. In the first case, three schemes for the piezoelectric actuation of various cantilevered panels, which differ in their geometrical layout, have been examined. The results have revealed that for a long panel, which is characterized by relatively large length to face sheet thickness ratio, the most effective actuation scheme is based on electrical extension and contraction of one of the face sheets (global bending). It has also been shown that adequate results can be achieved using a nonsymmetric actuation scheme, in which the piezoceramic layers are located at the core–face-sheet interfaces and protected by the soft core. On the other hand, for a short panel, which is characterized by relatively thick face sheets, it has been shown that the local bending actuation scheme yields the largest deflections. Yet, this configuration is associated with enhanced stresses in the face sheets and in the core.

The second numerical case has focused on the effect of electrical actuation using piecewise piezoceramic layers and compares the results to the response of a similar panel with continuous actuators. The results have indicated that the piecewise actuation is associated with smaller induced deformations; hence, it might be considered less effective. On the other hand, smaller peak internal stress resultants and smaller shear stresses in the core are also observed using the piecewise active layers.

The analytical formulation and the numerical results presented in this paper have revealed the broad range of possibilities for active shape control of sandwich panels with flexible cores. The analysis has also revealed the high-order response, the localized effects, and the stress concentrations associated with such actuation. The ability to predict these effects, as well as its generality and suitability to any combination of loading and boundary conditions, are among the major advantages of the proposed model.

Acknowledgment

Appreciation is expressed to the Center for Composite Materials, University of Delaware, for providing a postdoctoral fellowship to the first author during 2001–2002.

References

[1]Wang, Q., and Quek, S. T., "Flexural Vibration Analysis of Sandwich Beams Coupled with Piezoelectric Actuator," *Smart Materials and Structures*, Vol. 9, No. 1, 2000, pp. 103–109.

[2]Abramovich, H., and Pletner, B., "Actuation and Sensing of Piezolaminated Sandwich Type Structures," *Composite Structures*, Vol. 38, Nos. 1–4, 1998, pp. 17–27.

[3]Trindade, M. A., Benjeddou, A., and Ohayon, R., "Parametric Analysis of the Vibration Control of Sandwich Beams Through Shear–Based Piezoelectric Actuation," *Journal of Intelligent Material Systems and Structures*, Vol. 10, No. 5, 1997, pp. 377–385.

[4]Benjeddou, A., Trindade, M. A., and Ohayon, R., "Piezoelectric Actuation Mechanisms of Intelligent Sandwich Structures," *Smart Materials and Structures*, Vol. 3, No. 1, 2000, pp. 328–335.

[5]Benjeddou, A., Trindade, M. A., and Ohayon, R., "A Unified Beam Finite Element Model for Extension and Shear Piezoelectric Actuation Mechanism," *Journal of Intelligent Material Systems and Structures*, Vol. 8, No. 12, 1997, pp. 1012–1025.

[6]Bisegna, P., and Caruso, G., "Mindlin-Type Finite Element for Piezoelectric Sandwich Plates," *Journal of Intelligent Material Systems and Structures*, Vol. 11, No. 1, 1997, pp. 14–25.

[7]Zhang, X. D., and Sun, C. T., "Formulation for an Adaptive Sandwich Beam," *Smart Materials and Structures*, Vol. 5, No. 6, 1996, pp. 814–823.

[8]Zhang, X. D., and Sun, C. T., "Analysis of a Sandwich Plate Containing a Piezoelectric Core," *Smart Materials and Structures*, Vol. 8, No. 1, 1999, pp. 31–40.

[9]Wang, G., Veeramani, S., and Wereley, N. M., "Analysis of Sandwich Plates with Isotropic Face Plates and Viscoelastic Core," *Journal of Vibration and Acoustics*, Vol. 122, No. 2, 2000, pp. 305–312.

[10]Birman, V., "Analytical Model of Sandwich Plates with Piezoelectric Strip-Stiffeners," *International Journal of Mechanical Sciences,* Vol. 36, No. 6, 1994, pp. 567–578.

[11]Birman, V., and Simonyan, A., "Optimum Distribution of Smart Stiffeners in Sandwich Plates Subjected to Bending or Forced Vibrations," *Composites Part B: Engineering*, Vol. 27, No. 6, 1996, pp. 657–665.

[12]Frostig, Y., Baruch, M., Vilnai, O., and Sheinman, I., "High-Order Theory for Sandwich-Beam Bending with Transversely Flexible Core," *Journal of the Engineering Mechanics Division, ASCE*, Vol. 118, No. 5, 1992, pp. 1026–1043.

[13]Frostig, Y., and Baruch, M., "High-Order Buckling Analysis of Sandwich Beams with Transversely Flexible Core," *Journal of the Engineering Mechanics Division, ASCE*, Vol. 119, No. 3, 1993, pp. 476–495.

[14]Frostig, Y., "Buckling of Sandwich Panels with a Transversely Flexible Core—High-Order Theory," *International Journal of Solids and Structures*, Vol. 35, Nos. 3–4, 1998, pp. 183–204.

[15]Frostig, Y., "Behavior of Delaminated Sandwich Beams with Transversely Flexible Core—High Order Theory," *Composite Structures*, Vol. 20, No. 1, 1992, pp. 1–16.

[16]Frostig, Y., and Rabinovitch, O., "Behavior of Sandwich Panels with Multi-skin Construction or a Multi-layered Core—A High-Order Approach," *Journal of Sandwich Structures and Materials*, Vol. 2, No. 3, 2000, pp. 181–213.

[17]Thomsen, O. T., and Frostig, Y., "Localized Bending Effects in Sandwich Panels: Photoelastic Investigation Versus High-Order Sandwich Theory Results, *Composite Structures*, Vol. 37, No. 1, 1997, pp. 97–108.

[18]Tiersten, H. F., *Linear Piezoelectric Plate Vibrations*, Plenum, New York, 1969, pp. 45–50.

[19]Dym, C. L., and Shames, I. H., *Solid Mechanics, A Variational Approach*, McGraw–Hill, New York, 1973, pp. 65–108.

[20]Birkhoff, G., and Rota, G.-C., *Ordinary Differential Equations*, 2nd ed., Blaisdell, Waltham, MA, 1969, pp. 83–111.

K. N. Shivakumar
Associate Editor